JACS
JOURNAL OF THE AMERICAN CHEMICAL SOCIETY

Article

pubs.acs.org/JACS

Hydrogen Peroxide Displacing DNA from Nanoceria: Mechanism and Detection of Glucose in Serum

Biwu Liu, Ziyi Sun, Po-Jung Jimmy Huang, and Juewen Liu*

Department of Chemistry, Waterloo Institute for Nanotechnology, Waterloo, Ontario, Canada N2L 3G1

Supporting Information

ABSTRACT: Hydrogen peroxide (H_2O_2) is a key molecule in biology. As a byproduct of many enzymatic reactions, H_2O_2 is also a popular biosensor target. Recently, interfacing H_2O_2 with inorganic nanoparticles has produced a number of nanozymes showing peroxidase or catalase activities. CeO_2 nanoparticle (nanoceria) is a classical nanozyme. Herein, a fluorescently labeled DNA is used as a probe, and H_2O_2 can readily displace adsorbed DNA from nanoceria, resulting in over 20-fold fluorescence enhancement. The displacement mechanism instead of oxidative DNA cleavage is confirmed by denaturing gel electrophoresis and surface group pK_a measurement. This system can sensitively detect H_2O_2 down to 130 nM (4.4 parts-per-billion). When coupled with glucose oxidase, glucose is detected down to 8.9 μM in buffer. Detection in serum is also achieved with results comparable with that from a commercial glucose meter. With an understanding of the ligand role of H_2O_2, new applications in rational materials design, sensor development, and drug delivery can be further exploited.

INTRODUCTION

Hydrogen peroxide (H_2O_2) plays critical roles in a diverse range of biological processes including biosynthesis, host defense, and cell signaling.[1] An elevated H_2O_2 concentration often links to oxidative stress. In addition, being an incomplete reduction product of oxygen, H_2O_2 is a byproduct of many enzymatic reactions. The most well-known example is the oxidation of glucose by glucose oxidase (GOx), where H_2O_2 is the actual target molecule of most glucose sensors. For these reasons, detecting H_2O_2 has long attracted the interest of many chemists,[2] and a number of sensing methods were developed. For example, as a cosubstrate for peroxidases, H_2O_2 can be measured using chromogenic substrates such as Amplex Red or 3,3′,5,5′-tetramethylbenzidine (TMB). Intracellular detection relies on fluorescent probes that light up by reacting with H_2O_2. Recently, Chang and co-workers developed a series of boronate-based molecules that light up by H_2O_2 for cellular and in vivo imaging.[3]

Aside from these traditional methods, recent studies on nanozymes have produced a few new sensing approaches. Nanozymes are nanoparticles with enzyme-like properties.[4] For example, nanoceria (CeO_2 nanoparticle) possesses a few types of enzyme-like activities.[5−8] This is probably related to the coexistence of both Ce^{3+} and Ce^{4+} on the surface, where the Ce^{3+} species is coupled with oxygen vacancies. As an oxidase mimic, nanoceria oxidizes many common substrates including TMB.[9,10] It also has peroxidase, superoxide dismutase, and catalase activities under different conditions.[7,11] Its reaction with reactive oxygen species (ROS) makes it useful as an antioxidant.[12−15] When nanoceria is mixed with H_2O_2, its color changes to orange. Direct detection of H_2O_2 based on this color change was reported.[16] However, the sensitivity is limited since an obvious color change requires high concentrations of H_2O_2. In addition, a similar color change may arise by reacting nanoceria with other biological molecules such as ascorbate and dopamine.[17,18] These reactions may interfere with color-based detection.

With these progresses, our fundamental understanding on the interaction between H_2O_2 and nanoceria is still far from complete, which hinders further developments. While many spectroscopic methods have been used, we reason that DNA might be a simple probe to study surface interactions.[19] Since cerium is a hard metal that likes phosphate containing ligands, nanoceria strongly binds to DNA and nucleotides.[6,20] The tunable length and sequence of DNA also facilitates systematic studies.

Herein, we probed H_2O_2 and nanoceria interaction using DNA. Although H_2O_2 is often linked to oxidative DNA damages in the presence of redox metals (e.g., in the Fenton chemistry), we emphasize on a simple ligand role of H_2O_2, displacing adsorbed DNA without cleavage. This study contributes new knowledge to the interaction between H_2O_2 and inorganic surfaces and also expands the scope of DNA-based sensing.[19] With a DNA/nanoceria complex, we detected H_2O_2 and glucose (when coupled with the GOx) with very high sensitivity and selectivity.

MATERIALS AND METHODS

Chemicals. All of the DNA oligomers were purchased from Integrated DNA Technologies (IDT, Coralville, IA). The DNA sequences and modifications are listed in Supporting Information Table S1. Sodium acetate, sodium chloride, 4-(2-hydroxyethyl)-piperazine-1-ethanesulfonic acid (HEPES), 2-(*N*-morpholino)-ethanesulfonic acid (MES), and the nucleosides were from Mandel

Received: November 6, 2014
Published: January 9, 2015

DOI: 10.1021/ja511444e
J. Am. Chem. Soc. 2015, 137, 1290−1295

Scientific (Guelph, ON, Canada). Glucose, fructose, galactose, sucrose, 30 wt % H_2O_2 solution, dopamine, sodium ascorbate, amino acids, fetal bovine serum (FBS) and nanoceria dispersion (catalog number: 289744, 20% dispersed in 2.5% acetic acid) were from Sigma-Aldrich. For applications related to pH change measurement, the nanoceria sample was washed three times using ultracentrifugation. Milli-Q water was used for all the experiments.

Transmission Electron Microscopy (TEM), Dynamic Light Scattering (DLS), and UV–Vis Spectroscopy. The size and morphology of nanoceria were studied using TEM (Philips CM10). The sample was prepared by dropping nanoceria (10 μg/mL) on a copper grid. The UV–vis spectra of nanoceria were acquired using a UV–vis spectrometer (Agilent 8453A). For visual observation, nanoceria (1 mg/mL) was incubated with H_2O_2 (10 mM) for 15 min (recorded with a digital camera). The sample was diluted 25 times (40 μg/mL) for the UV–vis measurement. The hydrodynamic size and ζ-potential were measured using DLS at 25 °C (Malvern Nanosizer ZS90). To obtain pH-dependent ζ-potential, nanoceria (50 μg/mL) was dispersed in designed buffer solutions (acetate for pH 4 and 5, MES for pH 6, and HEPES for pH 7 and 8, 10 mM each).

DNA Adsorption Kinetics and Capacity. To study salt-dependent DNA adsorption, FAM-A_{15} (50 nM) was dissolved in HEPES buffer (pH 7.6, 10 mM) containing varying concentrations of NaCl. After the free DNA was scanned for 2 min (excitation at 485 nm, emission at 535 nm) using a microplate reader (Infinite F200Pro, Tecan), a small volume of nanoceria (final concentration = 3 μg/mL) was added to induce DNA adsorption. The fluorescence intensity was normalized based on the initial intensity before adding nanoceria. The DNA loading capacity as a function of pH was measured by comparing fluorescence before and after adding nanoceria (3 μg/mL) to an Alexa Fluor 488 labeled DNA (Alexa-DNA, 200 nM, see Supporting Information Table S1 for sequence).

H_2O_2-Induced DNA Desorption. Typically, the DNA–nanoceria conjugate was first prepared as described above. After recording the background, H_2O_2 was added to induce DNA desorption. In the NaCl concentration and pH dependent studies, the final concentration of H_2O_2 was 1 mM. To investigate the effect of DNA sequence and length, FAM-labeled DNA was adsorbed onto nanoceria (4 μg/mL) in buffer (HEPES 10 mM, pH 7.6, NaCl 150 mM). After 1 h incubation, H_2O_2 was added to release DNA. The fluorescence photo of H_2O_2-induced DNA release was taken under a UV lamp (365 nm excitation). FAM-A_{15} (200 nM) was used as the probe DNA and the final H_2O_2 concentration was 10 mM. To test the sensitivity for H_2O_2 detection, various concentrations of H_2O_2 (from 100 nM to 5 mM) were added to the FAM-T_5 DNA/nanoceria conjugate. The fluorescence intensity at 5 min after H_2O_2 addition was plotted as a function of H_2O_2 concentration. For selectivity test, the concentration of competing analytes was 1 mM (50 μM of sodium ascorbate was also tested).

Potentiometric Titration. Conductivity and pH were measured simultaneously using a Metrohm 809 Titrando autotitrator. The stock nanoceria and H_2O_2 treated nanoceria were centrifuged for 10 min (100 000 rpm) to remove the supernatant and then dispersed in Milli-Q water for three times. This is to remove the free acetic acid present in the original solution. Then, the pH of the nanoceria sample (0.1 wt %) was adjusted to ~3 by adding HCl. The sample was then titrated with 0.02 M NaOH until the pH approached a plateau. The pK_a values were calculated after taking the second derivative of the titration traces.

Gel Electrophoresis. The conjugate was prepared by mixing FAM-A_{30} (200 nM) and nanoceria (15 μg/mL) in HEPES buffer (pH 7.6, 10 mM, NaCl 150 mM) and 1 mM H_2O_2 was added to induce DNA desorption. Free DNA and DNA treated with H_2O_2 alone were also included for comparison. The samples were loaded in 10% denaturing polyacrylamide gel and were then imaged using a gel documentation system (Chemidoc MP, Bio-Rad).

pH Monitoring. Washed nanoceria (1.5 mg/mL, 0.15 wt %) was reacted with H_2O_2 (50 mM) and the pH of the solution was monitored by a pH meter for 2 h at various time points. In addition, the same reaction was carried out in 10 mM HEPES (pH 7.6, nanoceria = 3 μg/mL, H_2O_2 = 50 mM). To obtain the reaction kinetics of H_2O_2 decomposition, nanoceria (3 μg/mL) was added into 50 mM H_2O_2 solution. The UV–vis absorbance at 240 nm was then followed.

Glucose Detection. Detection of glucose in buffer was performed as the following steps: (1) various concentrations of glucose (from 10 to 500 μM) were, respectively, incubated with glucose oxidase (GOx, 50 μg/mL) in HEPES buffer (pH 7, 20 mM) at 37 °C for 40 min; (2) 50 μL of the solution after incubation was added into 50 μL DNA-nanoceria conjugate. The fluorescence intensity after 5 min was recorded. For the selectivity test, 5 mM fructose, galactose, and sucrose were, respectively, incubated with GOx in the same way. For sensing glucose in FBS, the standard addition method was used. Glucose was added into the FBS with varying concentration (0.5–6 mM). Then, 10 μL of FBS with or without additional glucose was added into 990 μL of HEPES buffer (pH 7, 20 mM) containing GOx (50 μg/mL) at 37 °C for 40 min. The calculated value was multiplied by 100 to obtain the glucose concentration in serum. A commercial glucose meter (BAYER, Contour next EZ) was also used to measure the glucose in FBS following the vendor recommended protocol.

RESULTS AND DISCUSSION

H_2O_2-Induced DNA Desorption. Our nanoceria has a size of ~5 nm as characterized by transmission electron microscopy (TEM, Supporting Information Figure S1A). Dynamic light scattering (DLS) indicates a similar average size with a relatively high polydispersity (Supporting Information Figure S1B). Upon addition of H_2O_2, the color of nanoceria changes from colorless to orange (inset of Figure 1C), which is reflected by UV–vis measurement (Figure 1C).[16,21] The increased absorption at ~400 nm explains the orange color, allowing H_2O_2 to be detected down to ~10 μM.[16] Due to the small UV–vis spectral shift and high background, we reason that better sensitivity might be achieved using fluorescence-based detection.

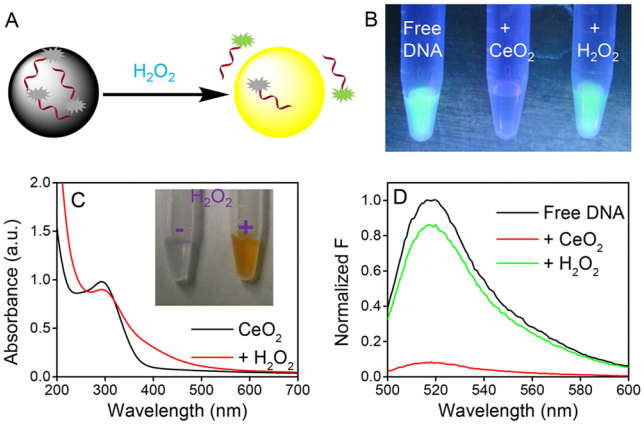

Figure 1. (A) Sensing H_2O_2 by displacing adsorbed fluorescent DNA from nanoceria. The color of nanoceria is changed in the same process. (B) A fluorescence photo of free FAM-A_{15} DNA (200 nM), after adding nanoceria (10 μg/mL) and then adding H_2O_2 (10 mM). (C) UV–vis spectra of untreated nanoceria (40 μg/mL) and after reacting with H_2O_2 (0.4 mM). Inset: a photo of the same samples (25× concentrated than the UV–vis sample). (D) Fluorescence spectra of the samples diluted from (B).

Figure 1B (left panel) shows the fluorescence image of a FAM (carboxyfluorescein) labeled DNA. After nanoceria was added, the fluorescence was completely quenched, suggesting DNA adsorption. Interestingly, fluorescence was fully and immediately recovered after adding H_2O_2. The fluorescence spectra of these samples are shown in Figure 1D. This proof-of-concept study indicates the possibility of using DNA-function-

DOI: 10.1021/ja511444e
J. Am. Chem. Soc. 2015, 137, 1290–1295

alized nanoceria to directly detect H_2O_2 (Figure 1A), which may allow much higher sensitivity compared to the colorimetric detection. At the same time, DNA can serve as a mechanistic probe to study the interaction between H_2O_2 and nanoceria.

Nanoceria is slightly negatively charged at neutral pH (ζ-potential = −6.2 mV). Efficient DNA adsorption occurred even in the absence of additional salt and complete adsorption was achieved with just 30 mM NaCl (Supporting Information Figure S2). This indicates a strong affinity between DNA and nanoceria. Such low background fluorescence is ideal for sensing since it allows a large signal increase and low noise.

After adsorbing DNA, the H_2O_2 signaling kinetics as a function of salt concentration were measured. All the samples maintained a stable background in the absence of H_2O_2 (Figure 2A). At 2 min, H_2O_2 was added. It is interesting to note that a higher salt concentration produced stronger fluorescence enhancement, while barely any fluorescence was generated in the absence of salt. It is unlikely that the interaction between nanoceria and H_2O_2 is affected by such low concentrations of NaCl. We reason that the salt effect is mainly acting on the DNA. With a higher ionic strength, DNA tends to adopt a more compact structure (e.g., screening intramolecular charge repulsion), thus reducing the number of contacting points on nanoceria and facilitating DNA desorption.

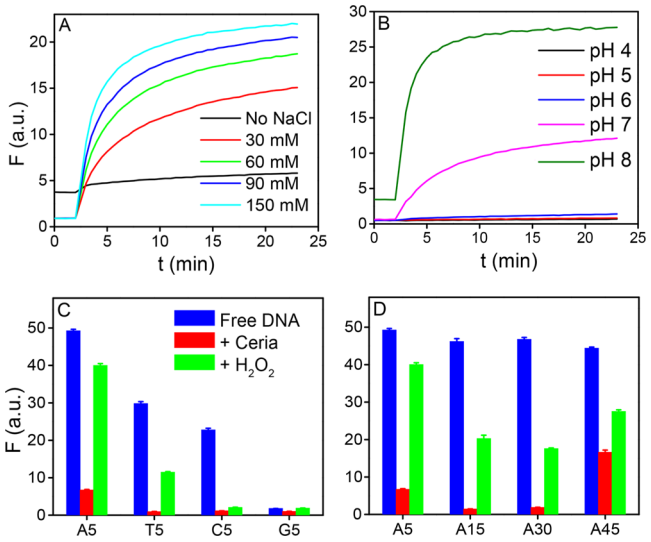

Figure 2. Desorption kinetics of (A) FAM-A_{15} by H_2O_2 (1 mM) as a function of salt concentration at pH 7.6 and (B) Alexa Fluor 488-labeled DNA at different pH (150 mM NaCl). Effect of (C) DNA sequence and (D) DNA length on H_2O_2 signaling (all with FAM labels). The error bars represent standard deviation from three independent measurements.

The effect of pH is also very pronounced (Figure 2B). H_2O_2 induces the fastest signaling at pH 8, and this first-order rate decreases by 4-fold at pH 7. Barely any fluorescence change occurs at pH 6 or lower. To understand this, we measured the ζ-potential of nanoceria as a function of pH, and the point of zero charge (POZ) is between pH 6 and 7 (Figure 3B, black dots). We reason that as the surface of nanoceria becomes more positively charged at lower pH, electrostatic attraction inhibits DNA release. Since pH 8 already shows some background signal, we did not test even higher pH. The optimal value should be between pH 7 and 8, which is ideal for detecting H_2O_2 in physiological conditions.

The effect of DNA sequence was studied next. Ideally, shorter DNA should be used, allowing higher probe density and thus better sensitivity. Therefore, 5-mer FAM-labeled DNAs were tested (Figure 2C). Since guanine is a quencher, FAM-G_5 has very low fluorescence intensity as a free DNA, while the other three give much stronger emission (blue bars). After adding nanoceria, T_5 and C_5 quenched most significantly (red bars). Fluorescence recovery was achieved after adding H_2O_2 for all the samples (green bars), but the increase with C_5 and G_5 was very moderate. Overall, A_5 and T_5 appear to be optimal.

To test the effect of DNA length, a few poly-A DNAs were employed (Figure 2D). More efficient adsorption was observed with A_{15} and A_{30} compared to A_5, possibly due to more interaction points, leading to stronger adsorption and lower background. However, A_{45} showed a high background and poor fluorescence recovery by H_2O_2, which might be related to its large size and some fluorophores are far away from the nanoceria surface even after DNA adsorption.

Signaling Mechanism. It is quite unexpected that H_2O_2 enhances the fluorescence. Two mechanisms may explain this: (1) oxidative DNA cleavage, or (2) H_2O_2-induced DNA desorption. H_2O_2 is reservoir for ROS and it can be converted to more reactive hydroxyl radicals in the presence of redox active metals to oxidatively cleave DNA (e.g., Fenton chemistry with Fe^{2+}). Given the redox property of cerium, oxidative DNA cleavage appears to be a quite possible mechanism.

To test this, a gel electrophoresis experiment was carried out (Figure 3A). The first lane is a ladder of 30, 15, and 5-mer FAM-labeled poly-A DNA. Lane 2 is the FAM-A_{30} DNA without any treatment. Lane 3 is the DNA incubated with 1 mM H_2O_2. Lane 4 is the DNA/nanoceria complex, and lane 5 is DNA/nanoceria treated with 1 mM H_2O_2, mimicking the sensing condition. However, no DNA cleavage was observed for any of these samples. Therefore, the oxidative DNA cleavage mechanism is ruled out and the reaction is likely to be simply H_2O_2-induced DNA desorption. In fact, some reports show that nanoceria can decrease the oxidative stress by reacting with ROS,[22] thus avoiding DNA cleavage. On the other hand, DNA cleavage was reported in some other systems. A recent example is cleavage in the presence of silver nanoparticles, graphene oxide and H_2O_2.[23]

To further confirm this, we reacted nanoceria with H_2O_2 first to produce the orange-colored product. The extra H_2O_2 was washed away after centrifugation and the particles remained orange. When DNA was added to this sample, the adsorption was significantly lower, especially at higher pH (Supporting Information Figure S3). This further indicates that it is the surface change of nanoceria that inhibits DNA adsorption (no free H_2O_2 required), instead of changes related to DNA.

The nanoceria surface becomes more negatively charged after the H_2O_2 treatment compared to the original nanoceria (e.g., POZ = ~5, Figure 3B). This could explain its decreased DNA binding affinity. To further understand the surface chemistry of CeO_2 after H_2O_2 treatment, a pH and conductivity titration experiment was performed to measure the pK_a of surface groups on nanoceria. Untreated nanoceria has a pK_a of 8.62, while after the H_2O_2 treatment, two pK_a's were observed (see Supporting Information Figure S4 for the titration traces). The one at 8.85 is similar to the untreated sample, and the other value is 7.61. This new and more acidic group on nanoceria after the H_2O_2 treatment explains the shift of the POZ to lower pH from the ζ-potential measurement in Figure 3B.

DOI: 10.1021/ja511444e
J. Am. Chem. Soc. 2015, 137, 1290−1295

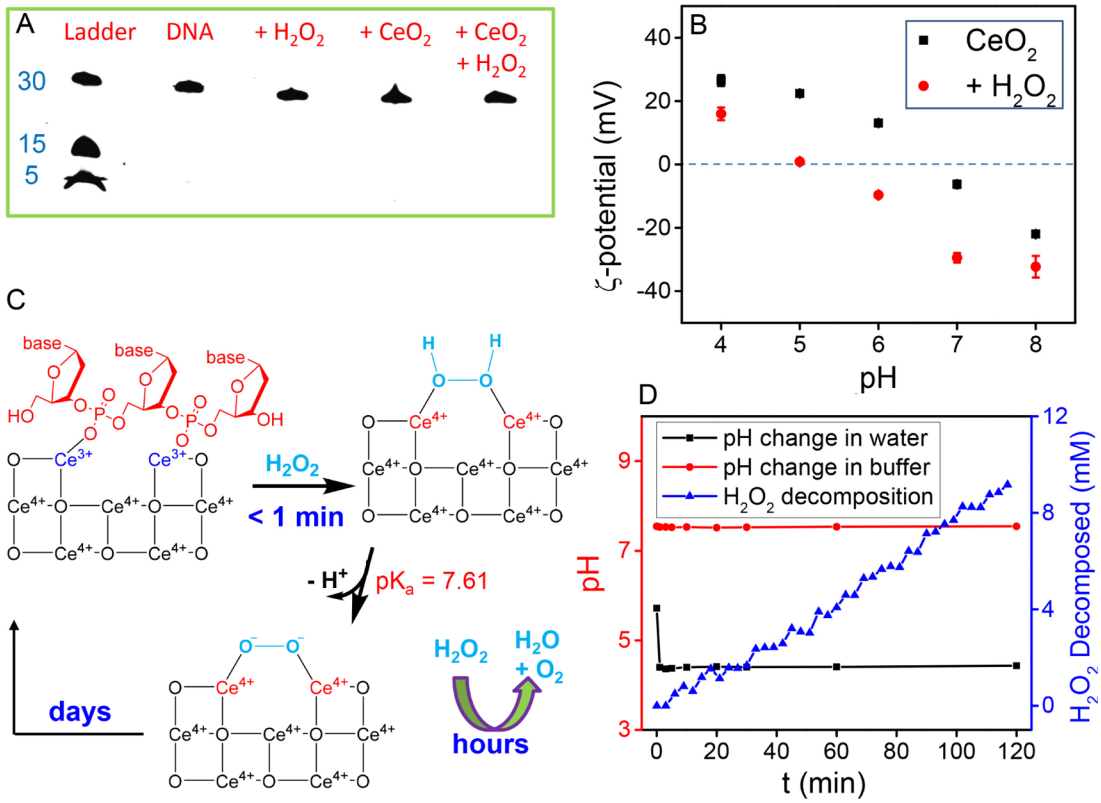

Figure 3. (A) Gel electrophoresis to check DNA integrity. [H_2O_2] = 1 mM. (B) ζ-potential of nanoceria as a function of pH in the absence and presence of H_2O_2. (C) A proposed mechanism of H_2O_2-induced DNA release by capping the nanoceria surface. For the three time scales marked in the scheme, DNA release is related to the one on the order of 1 min. (D) Kinetics of pH change after mixing H_2O_2 and nanoceria (1.5 mg/mL) in water or in 10 mM HEPES (pH 7.6) (left axis) and kinetics of H_2O_2 decomposition with 3 μg/mL nanoceria (right axis).

To further explore the mechanism of DNA desorption, we followed pH change in a nonbuffered solution. After mixing H_2O_2 and nanoceria, pH dropped by ~1 unit in less than 1 min (black squares, Figure 3D), and this initial pH drop was also observed by others.[24] This time scale agrees with that for the color change and DNA desorption. It is generally accepted that the color change is due to oxidation of Ce^{3+} to Ce^{4+}.[7,15,16,25] However, the pH drop cannot be explained by direct oxidation by H_2O_2. Instead, pH should increase if H_2O_2 is used to oxidize Ce^{3+} (e.g., $H_2O_2 + 2H^+ + 2e^- \rightarrow 2H_2O$). This pH change is very moderate (equal to producing ~40 μM protons), and is completely masked by 10 mM HEPES at our sensing conditions (red dots, Figure 3D). We reason this initial pH drop might be due to the remaining acetic acid in our nanoceria sample or nanoceria reacting with a trace amount of OH radicals.[26]

We also monitored the rate of H_2O_2 decomposition using UV−vis spectrometry (Figure 3D, blue triangles). In 2 h, ~10 mM H_2O_2 was decomposed with 3 μg/mL nanoceria (the rate is faster with more nanoceria). Therefore, H_2O_2 decomposition does not involve pH change.[14,24] Ghibelli and co-workers proposed a Ce^{4+}/Ce^{3+} cycle for H_2O_2 decomposition.[14] However, based on a rigorous spectroscopy study, Cafun et al. argued that the catalase activity of nanoceria does not involve discrete Ce^{3+} centers;[24] Ce^{4+} species in the whole particle acts as an electron sponge to perform catalysis.

Taken together, we reason that after adding H_2O_2, Ce^{3+} is quickly oxidized Ce^{4+}, yielding the orange color. The Ce^{4+} surface is further capped by H_2O_2 (Figure 3C), producing a more acidic peroxo proton (pK_a = 7.61). This capping reaction on one hand shields the cerium center from DNA phosphate binding, and on the other hand, increases the negative charge density. The peroxo ligand was reported in small molecule cerium complexes as well.[27] It was also reported that phosphate affinity with Ce^{4+} is much weaker than that with Ce^{3+}.[28] All these factors favor DNA desorption. Note that DNA desorption occurs in the first minute. Once desorbed, further decomposition of H_2O_2 should proceed as in the case of free nanoceria. The peroxo capped species is relatively stable. After consuming all H_2O_2, it slowly converts back to the original light colored state over many days.[24,26]

H_2O_2 Detection. After the mechanistic work, we next tested this system as a biosensor for H_2O_2. With the use of FAM-T_5 as a probe, the fluorescence intensity was followed after adding various concentrations of H_2O_2 (Figure 4A). With a high concentration of H_2O_2 (e.g., 1 mM), saturated signal was achieved in less than 1 min. The signal-to-background ratio reaches >20-fold, and over 80% of adsorbed DNA can be released. The fluorescence intensity at 5 min is plotted as a function of the H_2O_2 concentration (Figure 3B). The dynamic range reaches ~1 mM H_2O_2, and the detection limit is 130 nM H_2O_2 (4.4 ppb, 3σ/slope, inset). This is one of the most sensitive sensors for H_2O_2 based on nanoparticle optical detection (e.g., ~80-fold more sensitive than the previous colorimetric detection). For selectivity test, we measured a few common metabolites (1 mM each, Figure 4C). Only ascorbate gave an obvious signal, but 50 μM ascorbate (the physiological concentration) is silent, indicating highly specificity.

Glucose Detection. Given the sensor performance for H_2O_2, we next tested glucose detection. H_2O_2 was *in situ*

DOI: 10.1021/ja511444e
J. Am. Chem. Soc. 2015, 137, 1290−1295

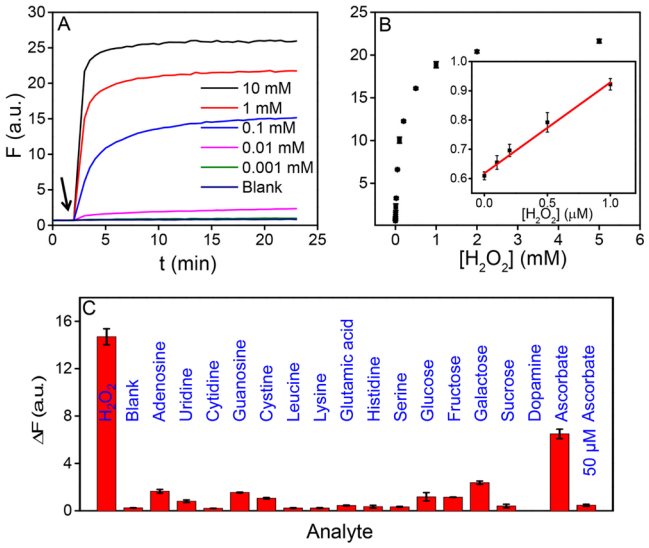

Figure 4. (A) Kinetics of sensor signaling. Arrowhead indicates H_2O_2 addition. (B) Sensor calibration curve. Inset: the initial linear response. (C) Selectivity test of H_2O_2 detection toward sugars, L-amino acids, nucleosides, and other metabolites (1 mM). The last bar is ascorbate at 50 μM.

generated using GOx and glucose. When the glucose concentration was varied, a linear response was observed with a detection limit of 8.9 μM glucose in buffer (Figure 5A). Only glucose produced signal, while the other sugars were silent (Figure 5B), consistent with the high specificity of GOx. Finally, we challenged the sensor by glucose measurement in blood serum. A commercial glucose meter was used to determine the concentration of glucose in undiluted serum and a value of 4.57 ± 0.06 mM was obtained. The serum was then analyzed by our sensor based on the GOx reaction. Due to its opaque optical appearance, we diluted the serum in buffer. Since our sensor is highly sensitive, accurate measurement was still possible after dilution. The standard addition method was used to minimize the sample matrix effect and a value of 4.37 ± 0.32 mM was obtained (Figure 5C, see Supporting Information Figure S5 for the titration curve). Within the error range, this result is the same as that from the glucose meter, indicating this sensor works in complex sample matrix.

CONCLUSIONS

In summary, by studying the interaction between H_2O_2 and nanoceria using DNA as a probe, we developed a highly sensitive sensor for H_2O_2. H_2O_2 acts as a capping ligand and it quickly releases DNA from the particle surface, generating fluorescence signal for H_2O_2. The effect of DNA length, sequence, salt concentration, and pH has been systematically studied. When coupled with GOx, it is possible to detect glucose even in blood serum samples. This study opens up many new ways of using H_2O_2 for interfacing with inorganic nanoparticles, and also expands the scope of DNA-based biosensors.

ASSOCIATED CONTENT

Supporting Information

TEM, DLS of nanoceria, control experiments, and pH titration traces. This material is available free of charge via the Internet at http://pubs.acs.org.

AUTHOR INFORMATION

Corresponding Author

liujw@uwaterloo.ca

Notes

The authors declare no competing financial interest.

ACKNOWLEDGMENTS

Funding for this work is from the University of Waterloo, the Canadian Foundation for Innovation, and Natural Sciences and Engineering Research Council of Canada (NSERC). J. Liu receives Early Researcher Award from the Ontario Ministry of Research and Innovation.

REFERENCES

(1) (a) Rhee, S. G. *Science* **2006**, *312*, 1882. (b) Giorgio, M.; Trinei, M.; Migliaccio, E.; Pelicci, P. G. *Nat. Rev. Mol. Cell. Biol.* **2007**, *8*, 722.
(2) (a) Gomes, A.; Fernandes, E.; Lima, J. L. F. C. *J. Biochem. Biophys. Methods* **2005**, *65*, 45. (b) Chen, X. Q.; Tian, X. Z.; Shin, I.; Yoon, J. *Chem. Soc. Rev.* **2011**, *40*, 4783. (c) Rhee, S. G.; Chang, T. S.; Jeong, W.; Kang, D. *Mol. Cells* **2010**, *29*, 539. (d) Song, Y. J.; Wei, W. L.; Qu, X. G. *Adv. Mater.* **2011**, *23*, 4215.
(3) Lippert, A. R.; Van de Bittner, G. C.; Chang, C. J. *Acc. Chem. Res.* **2011**, *44*, 793.
(4) (a) Kotov, N. A. *Science* **2010**, *330*, 188. (b) Lin, Y. H.; Ren, J. S.; Qu, X. G. *Acc. Chem. Res.* **2014**, *47*, 1097. (c) Wei, H.; Wang, E. *Chem. Soc. Rev.* **2013**, *42*, 6060. (d) Manea, F.; Houillon, F. B.; Pasquato, L.; Scrimin, P. *Angew. Chem., Int. Ed.* **2004**, *43*, 6165. (e) Luo, W.; Zhu, C.; Su, S.; Li, D.; He, Y.; Huang, Q.; Fan, C. *ACS Nano* **2010**, *4*, 7451. (f) Zheng, X.; Liu, Q.; Jing, C.; Li, Y.; Li, D.; Luo, W.; Wen, Y.; He, Y.; Huang, Q.; Long, Y.-T.; Fan, C. *Angew. Chem., Int. Ed.* **2011**, *50*, 11994. (g) Gao, L.; Zhuang, J.; Nie, L.; Zhang, J.; Zhang, Y.; Gu, N.; Wang, T.; Feng, J.; Yang, D.; Perrett, S.; Yan, X. *Nat. Nanotechnol.* **2007**, *2*, 577. (h) Li, Y.; He, X.; Yin, J.-J.; Ma, Y.; Zhang, P.; Li, J.;

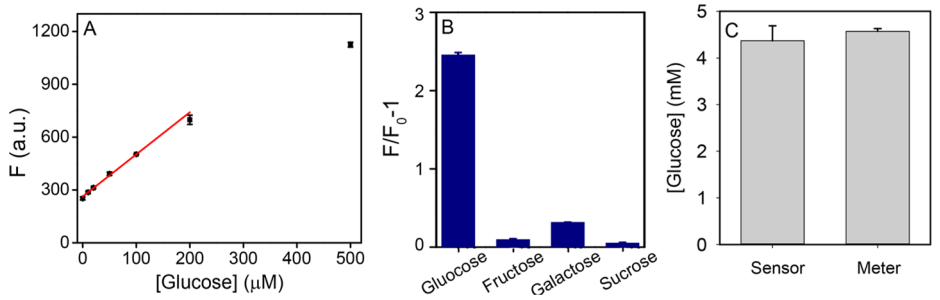

Figure 5. (A) Sensor calibration curve for glucose detection in buffer. (B) Sensor selectivity test for glucose detection in buffer. Glucose concentration = 0.5 mM and the other sugars are 5 mM. (C) Detection of glucose in serum by the nanoceria/DNA based sensor and by a commercial glucose meter.

DOI: 10.1021/ja511444e
J. Am. Chem. Soc. 2015, 137, 1290−1295

Ding, Y.; Zhang, J.; Zhao, Y.; Chai, Z.; Zhang, Z. *Angew. Chem., Int. Ed.* **2014**, DOI: 10.1002/anie.201410398.
(5) Lin, Y.; Xu, C.; Ren, J.; Qu, X. *Angew. Chem., Int. Ed.* **2012**, *51*, 12579.
(6) Xu, C.; Liu, Z.; Wu, L.; Ren, J.; Qu, X. *Adv. Funct. Mater.* **2014**, *24*, 1624.
(7) Xu, C.; Qu, X. *NPG Asia Mater.* **2014**, *6*, e90.
(8) Ujjain, S. K.; Das, A.; Srivastava, G.; Ahuja, P.; Roy, M.; Arya, A.; Bhargava, K.; Sethy, N.; Singh, S. K.; Sharma, R. K.; Das, M. *Biointerphases* **2014**, *9*, 031011.
(9) Asati, A.; Santra, S.; Kaittanis, C.; Nath, S.; Perez, J. M. *Angew. Chem., Int. Ed.* **2009**, *48*, 2308.
(10) Peng, Y.; Chen, X.; Yi, G.; Gao, Z. *Chem. Commun.* **2011**, *47*, 2916.
(11) (a) Chen, J.; Patil, S.; Seal, S.; McGinnis, J. F. *Nat. Nanotechnol.* **2006**, *1*, 142. (b) Pirmohamed, T.; Dowding, J. M.; Singh, S.; Wasserman, B.; Heckert, E.; Karakoti, A. S.; King, J. E. S.; Seal, S.; Self, W. T. *Chem. Commun.* **2010**, *46*, 2736. (c) Korsvik, C.; Patil, S.; Seal, S.; Self, W. T. *Chem. Commun.* **2007**, 1056.
(12) Menchón, C.; Martín, R.; Apostolova, N.; Victor, V. M.; Álvaro, M.; Herance, J. R.; García, H. *Small* **2012**, *8*, 1895.
(13) Karakoti, A. S.; Singh, S.; Kumar, A.; Malinska, M.; Kuchibhatla, S. V. N. T.; Wozniak, K.; Self, W. T.; Seal, S. *J. Am. Chem. Soc.* **2009**, *131*, 14144.
(14) Celardo, I.; Pedersen, J. Z.; Traversa, E.; Ghibelli, L. *Nanoscale* **2011**, *3*, 1411.
(15) Lee, S. S.; Song, W. S.; Cho, M. J.; Puppala, H. L.; Nguyen, P.; Zhu, H. G.; Segatori, L.; Colvin, V. L. *ACS Nano* **2013**, *7*, 9693.
(16) Ornatska, M.; Sharpe, E.; Andreescu, D.; Andreescu, S. *Anal. Chem.* **2011**, *83*, 4273.
(17) Hayat, A.; Andreescu, D.; Bulbul, G.; Andreescu, S. *J. Colloid Interface Sci.* **2014**, *418*, 240.
(18) Sharpe, E.; Frasco, T.; Andreescu, D.; Andreescu, S. *Analyst* **2013**, *138*, 249.
(19) (a) Wang, H.; Yang, R. H.; Yang, L.; Tan, W. H. *ACS Nano* **2009**, *3*, 2451. (b) Liu, J.; Cao, Z.; Lu, Y. *Chem. Rev.* **2009**, *109*, 1948. (c) Rosi, N. L.; Mirkin, C. A. *Chem. Rev.* **2005**, *105*, 1547. (d) Li, D.; Song, S. P.; Fan, C. H. *Acc. Chem. Res.* **2010**, *43*, 631. (e) Zhang, H.; Li, F.; Dever, B.; Li, X.-F.; Le, X. C. *Chem. Rev.* **2013**, *113*, 2812. (f) Du, Y.; Li, B. L.; Wang, E. K. *Acc. Chem. Res.* **2013**, *46*, 203. (g) Freeman, R.; Girsh, J.; Willner, I. *ACS Appl. Mater. Interfaces* **2013**, *5*, 2815. (h) Zhao, W.; Brook, M. A.; Li, Y. *ChemBioChem* **2008**, *9*, 2363. (i) Pu, F.; Ren, J.; Qu, X. *Adv. Mater.* **2014**, *26*, 5742. (j) Liu, J. *Phys. Chem. Chem. Phys.* **2012**, *14*, 10485.
(20) Pautler, R.; Kelly, E. Y.; Huang, P.-J. J.; Cao, J.; Liu, B.; Liu, J. *ACS Appl. Mater. Interfaces* **2013**, *5*, 6820.
(21) Lang, N. J.; Liu, B.; Liu, J. *J. Colloid Interface Sci.* **2014**, *428*, 78.
(22) Xue, Y.; Zhai, Y. W.; Zhou, K. B.; Wang, L.; Tan, H. N.; Luan, Q. F.; Yao, X. *Chem.—Eur. J.* **2012**, *18*, 11115.
(23) Wang, L.; Zheng, J.; Li, Y.; Yang, S.; Liu, C.; Xiao, Y.; Li, J.; Cao, Z.; Yang, R. *Anal. Chem.* **2014**, *86*, 12348.
(24) Cafun, J.-D.; Kvashnina, K. O.; Casals, E.; Puntes, V. F.; Glatzel, P. *ACS Nano* **2013**, *7*, 10726.
(25) (a) Sardesai, N. P.; Andreescu, D.; Andreescu, S. *J. Am. Chem. Soc.* **2013**, *135*, 16770. (b) Das, M.; Patil, S.; Bhargava, N.; Kang, J.-F.; Riedel, L. M.; Seal, S.; Hickman, J. J. *Biomaterials* **2007**, *28*, 1918.
(26) Perez, J. M.; Asati, A.; Nath, S.; Kaittanis, C. *Small* **2008**, *4*, 552.
(27) (a) Mingos, D. M. P. *Nature* **1971**, *230*, 154. (b) Wang, G.-C.; Sung, H. H. Y.; Williams, I. D.; Leung, W.-H. *Inorg. Chem.* **2012**, *51*, 3640. (c) Mustapha, A.; Reglinski, J.; Kennedy, A. R. *Inorg. Chim. Acta* **2009**, *362*, 1267.
(28) McCormack, R. N.; Mendez, P.; Barkam, S.; Neal, C. J.; Das, S.; Seal, S. *J. Phys. Chem. C* **2014**, *118*, 18992.

DOI: 10.1021/ja511444e
J. Am. Chem. Soc. 2015, 137, 1290−1295